

All-Angle Phase Matching Condition and Backward Second-Harmonic Localization in Nonlinear Photonic Crystals

Emmanuel Centeno, Didier Felbacq, and David Cassagne

GES UMR-CNRS 5650 Université Montpellier II, Place E. Bataillon, CC074, 34095 Montpellier, France

(Received 7 September 2006; published 29 June 2007)

We demonstrate an isotropic phase matching in properly designed nonlinear two-dimensional photonic crystals. In addition, by combining left- and right-handed properties at the fundamental and second-harmonic frequencies, we obtain a backward second-harmonic generation. These two properties lead to an unusual second-harmonic localization effect in perfect lattice photonic crystals.

DOI: [10.1103/PhysRevLett.98.263903](https://doi.org/10.1103/PhysRevLett.98.263903)

PACS numbers: 42.70.Qs, 42.65.Ky

Photonic crystals (PCs) are periodic materials that offer new perspectives for manipulating light at the nanometer scale [1]. The index periodicity in several directions of space produces a large variety of optical effects that open routes for designing integrated photonic components [2]. For example, strong light confinement inside compact PC devices enhances the nonlinear material feedback [3,4]. In this scheme, high second-harmonic conversion is expected in the case of fundamental and/or second-harmonic resonances in microcavities [5–9]. Another means for efficient second-harmonic generation is to realize the so-called phase matching condition in PCs. Efficient second-harmonic emission requires the same optical index for both the fundamental field (FF) and the second-harmonic field (SHF). Unfortunately, semiconductor materials used in PC technology are strongly dispersive and optically isotropic. This optical index mismatch Δn is quantified by the coherence length $L_c = \frac{\lambda}{4\Delta n}$ [10]. The energy conversion being a growing function of L_c , efficient conversion requires a large value of L_c . In semiconductors illuminated with a FF around $1\ \mu\text{m}$, the order of magnitude of L_c is of the micron scale, which leads to low second-harmonic intensity level. However, the richness of the PC dispersion bands permits to compensate the optical material dispersion. An effective phase matching [11–13] can be obtained when both fundamental and second-harmonic Bloch wave vectors satisfy the relation: $\mathbf{k}_{2\omega} = 2\mathbf{k}_\omega$, which represents a constraint on the wavelength and on the incident angle. In that case, L_c tends to infinity and the second-harmonic conversion is optimized. Finally, the combination of both phase matching and high electromagnetic fields confinement leads to giant conversion inside finite height 2D-PCs [4,13] or to second-harmonic conversion increasing as the fifth power of the length in 1D PCs [14].

Up to now, the phase matching conditions could be reached in specific propagation directions only. In this Letter, we demonstrate that nearly perfect effective phase matching can be achieved in all propagation directions inside adequately designed 2D-PCs. Moreover, this all-angle effective phase matching condition can be extended

from the blue to the red second-harmonic emission by a simple scaling of the lattice constant. This unusual property offers more flexibility for the design of compact frequency converters in achieving the phase matching by simply selecting the fundamental frequency whatever the incident angle.

In addition, we demonstrate a novel SHF localization effect obtained inside a perfect lattice PC. The structure we used presents left-handed (LH) and right-handed (RH) properties at the fundamental and second-harmonic frequencies, respectively. The combination of ω -LH/ 2ω -RH properties leads to a backward second-harmonic emission. This unusual second-harmonic process characterized by a SHF propagating in the opposite direction with respect to the FF has recently been theoretically predicted in nonlinear left-handed metamaterials at microwave regime [15,16]. Here, we demonstrate a SHF localization mechanism in the visible spectrum that does not require trapping either the FF or the SHF inside a PC microcavity.

First, we focus on the all-angle phase matching in a 2D-PC. It is known that the propagation properties of PCs are obtained through the dispersion band analysis. In particular, the computation of the dispersion surfaces and the isofrequency curves allows the understanding of unusual refraction behaviors. In general, the dispersion relations between the wave vector and the frequency are anisotropic. Here, the challenge consists in fulfilling two crucial points. (1) The dispersion curves should be isotropic in order to phase match both FF and SHF whatever the propagation direction. In that case, we can define an effective phase index [17] at both frequencies by: $n_{\text{eff}}(\omega) = \frac{|\mathbf{k}_\omega|c}{\omega}$ (where ω is the pulsation and c the light velocity in vacuum). (2) Both effective phase indices should be equal, $n_{\text{eff}}(\omega) = n_{\text{eff}}(2\omega)$, in order to have an optimal second-harmonic conversion.

We have found that both criteria are simultaneously fulfilled in a 2D-PC consisting of a hexagonal array (lattice constant a) of airholes (radius r) etched in GaN (in the x - y plane). We first demonstrate this approach for a SHF emission at $\lambda/2 = 0.5\ \mu\text{m}$. By using the MIT-Photonic BANDS package [18] for TM polarized light and for a fixed

filling ratio, two sets of dispersion diagrams are computed with the GaN indices [19] calculated at both fundamental and second-harmonic frequencies (the indices are equal to 2.33 and 2.41 at $1\ \mu\text{m}$ and $0.5\ \mu\text{m}$, respectively), see the inset of Fig. 1. Then, we look for a couple of bands satisfying both criteria (1) and (2) for the considered frequencies. We have found that for the particular airholes radius $r = 0.425a$, an isotropic effective phase matching between the second and the eighth bands is achieved around $a/\lambda = 0.511$. This computation enables to determine the lattice constant of the crystal ($a = 551\ \text{nm}$) and then the airhole radius. This scheme has to be repeated for each considered frequencies and permits to determine the necessary PCs parameters satisfying the isotropic phase matching condition. A simple representation of this effective phase matching is obtained by plotting the dispersion surface of the eighth band on the same drawing as for the second band but for both half frequencies and $\mathbf{k}_{2\omega}$ vectors. In Fig. 1, we remark that the eighth band cuts the FF surface in a circular curve for the normalized frequency $a/\lambda = 0.511$. Therefore, at the fundamental wavelength $\lambda = 1\ \mu\text{m}$, the FF and SHF are almost perfectly phase matched in all directions. Hexagonal lattices with large filling factor present highly symmetrical Brillouin zone leading to quasi-isotropic dispersion diagrams for a wide frequency range. These properties are crucial for satisfying both criteria (1) and (2). However, the weak anisotropy of the dispersion curves (less than 1%) produces a small

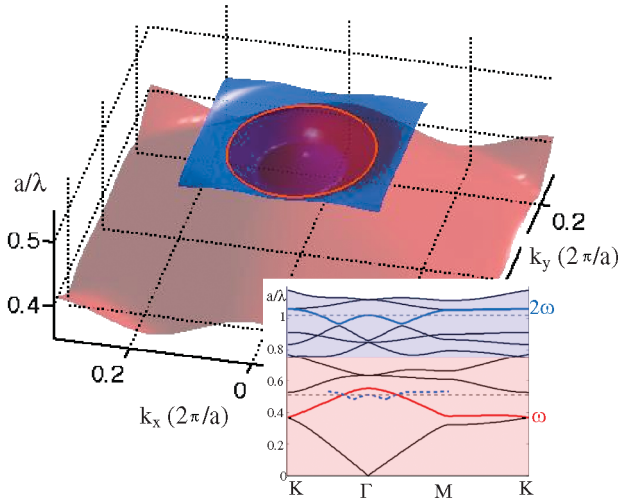


FIG. 1 (color). Dispersion surfaces of the second (red) and eighth (blue) bands. The circular intersection (red line) is the isofrequency curve presenting the all-angle phase matching condition. The inset represents the dispersion diagram where the four first bands are computed for the GaN index at $1\ \mu\text{m}$ (red area) and the higher bands for the index at $0.5\ \mu\text{m}$ (blue area). The dashed lines represent the frequency regime presenting the phase matching condition. The phase matching condition corresponds to the intersection points of the eighth band plotted for both half frequencies (dashed blue curve) and \mathbf{k} vectors and the second band (red curve).

mismatch quantified by the coherence length $L_c = \frac{\lambda}{4|n_{\text{eff}}(2\omega) - n_{\text{eff}}(\omega)|}$. In Fig. 2, the effective indices variation between ΓK and ΓM directions are plotted: they are exactly equal in an intermediate direction. The index mismatch in the crystalline directions leads to a coherent length larger than $1200\ \mu\text{m}$ and that approaches infinity when the effective phase matching is satisfied. From Fig. 2, it can be estimated that L_c is larger than $2000\ \mu\text{m}$ for 60% of the propagation directions. This giant coherent length larger than the typical size of the PC devices usually designed ($<100\ \mu\text{m}$) enables one to consider that this all-angle phase matching is perfect. Moreover, the PC dispersion properties balance the GaN index dispersion in all the visible SHF emission spectrum. A simple scaling the lattice constant with a constant filling ratio enables to extend the all-angle phase matching from the blue to the red second-harmonic generation, see Table I.

Beyond the versatility of 2D-PCs in achieving isotropic phase matching, the combination of opposite curvature dispersion surfaces leads to a backward second-harmonic generation. Indeed, at the considered normalized frequency ($a/\lambda = 0.511$), the \mathbf{k} vectors and the group velocities \mathbf{v}_g are antiparallel for the second band while they are parallel for the eighth band. Hence this 2D-PC behaves as a $\omega\text{-LH}/2\omega\text{-RH}$ system [20]. In the phase matching configuration both SHF and FF \mathbf{k} vectors are parallel; hence, the associated group velocities are antiparallel. Finally, both FF and SHF propagate in opposite directions inside a left- and a right-handed media, respectively. We illustrate this nonlinear effect inside a $6 \times 14\ \mu\text{m}$ 2D-PC constituted by a hexagonal array of airholes ($a = 511\ \text{nm}$ and $r = 217\ \text{nm}$) and satisfying the all-angle phase matching condition. We assume that the axis (001) of the GaN crystal is perpendicular to the airholes plane. In that case and for TM polarized fields, the term of the susceptibility tensor that contributes to the SH generation process is $\chi^{(2)}_{zzz}$

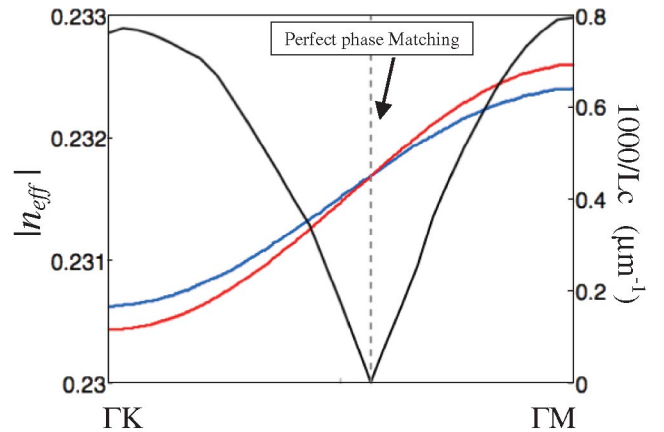


FIG. 2 (color). Effective phase indices for the FF (red) and the SHF (blue). The phase matching condition is satisfied between ΓM and ΓK directions. The black curve represents the variation of $1000/L_c$ in μm^{-1} unit with the propagation directions.

TABLE I. Lattice constants and GaN optical indices for blue and red all-angle phase matching. The airholes radius is fixed to $r = 0.425a$.

Second-harmonic wavelength	GaN indices	Lattice constant
400 nm	$n(800 \text{ nm}) = 2.34$	398 nm
	$n(400 \text{ nm}) = 2.54$	
750 nm	$n(1500 \text{ nm}) = 2.32$	774 nm
	$n(750 \text{ nm}) = 2.35$	

which is about 11 pm/V. A Gaussian beam propagating in the negative y direction at the fundamental wavelength $1 \mu\text{m}$ illuminates the PC in the ΓM direction. The second-harmonic emission is computed by using a multiple scattering method recently generalized to the parametric field conversion problem [21]. In Fig. 3(a), a periodic pattern due to multiple reflections at the PC interfaces (Fabry-Perot resonance) is observed for the FF. This FF is characterized by a group velocity pointing in the negative y direction and an opposite \mathbf{k} vector. In Fig. 3(b), the phase matched SHF is plotted: its pattern presents the same spatial periodicity as for the FF. Indeed, the second-harmonic emission is generated in the PC areas where the FF magnitude is high. We also note that the magnitude of the SHF increases linearly inside the PC, which corresponds to the classical quadratic growth of the second-harmonic efficiency observed in phase matched homogeneous media [10]. However, in accordance to the previous analysis, the SHF propagates in a direction opposite to the FF. This 2D-PC behaves as an effective mirror reflecting the SHF generated by an incoming FF [15,16].

An even more interesting effect is achieved by considering an internal source emitting a FF inside an isotropic phase matched $\omega\text{-LH}/2\omega\text{-RH}$ system. It is known that the introduction of PC lattice defects produces localized states with high energy density that enhance the conversion in single or doubly resonant microcavities [5–9]. Here, we use the backward second-harmonic generation in order to confine the SHF in a restricted PC area without the use of lattice defects. In Fig. 4(a), a wire antenna positioned at the center of the PC emits an isotropic FF at $\lambda = 1 \mu\text{m}$ (the PC parameters are the same as those used in the previous result). As discussed previously, at the fundamental frequency, this PC behaves as a LH medium: the FF radiates outward the PC but with a \mathbf{k} vector pointing toward the antenna, see Fig. 4(a). Therefore, the phase matched SHF has also \mathbf{k} vector pointing toward the wire antenna, which leads to a second-harmonic efficiency growth directed toward the FF emitter, see Fig. 4(b). We observe that the SHF is confined inside a cylindrical area of radius smaller than $1 \mu\text{m}$. However, contrary to previous cases presenting an external incoming pump field [Fig. 3(a) and 3(b)], here both FF and SHF group velocities are collinear. This phenomenon proceeds in fact from an interferential effect combining a backward phase matched field (with \mathbf{k} and \mathbf{v}_g pointing toward the antenna) and a forward field (with

outward \mathbf{k} and \mathbf{v}_g) propagating the energy accumulated at the center of the device. Finally, the SHF is a localized wave with a maximal magnitude condensed in a small area (less than two lattice periods) and satisfying the outgoing wave condition. This SHF localization effect is character-

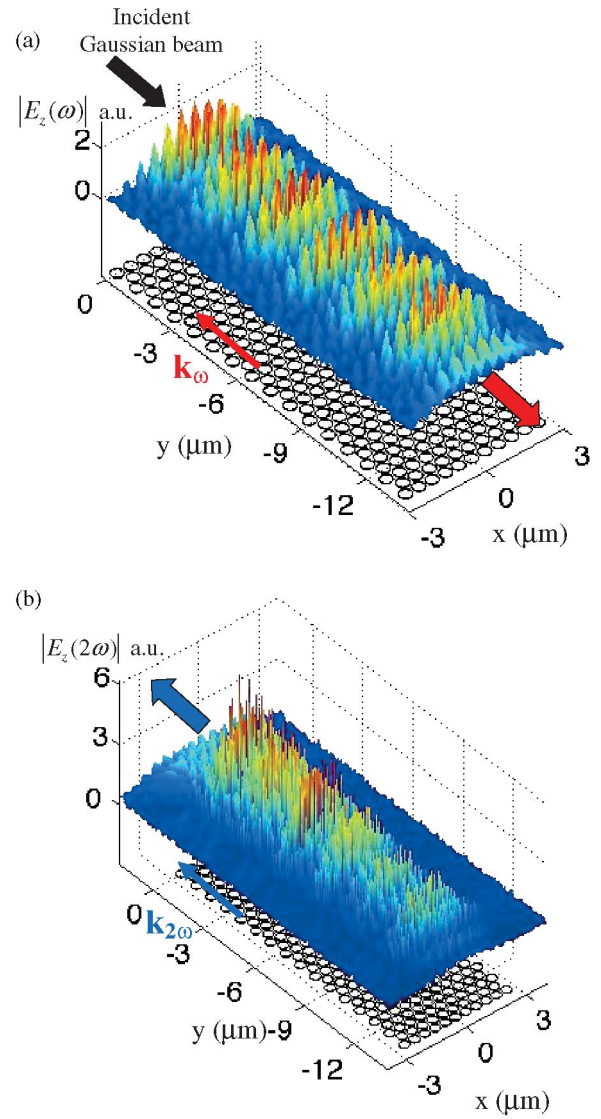


FIG. 3 (color). (a), (b) represent the modulus of the electric fields for the fundamental and second-harmonic frequencies, respectively. The large arrows indicate the propagation directions of both FF and SHF.

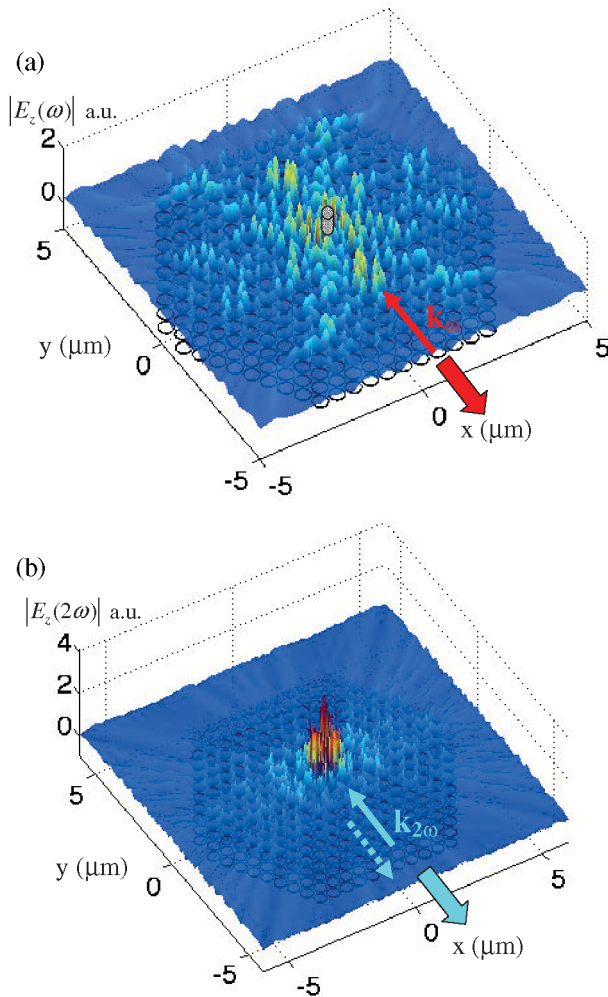


FIG. 4 (color). (a), (b) represent the modulus of FF and SHF, respectively, inside a hexagonal 2D PC. In (a), the red wire represents the FF emitter. In (b), the localized SHF combines two opposite waves: a backward wave with a \mathbf{k} vector pointing toward the emitter (blue thin arrow) and a forward wave (dashed thin arrow).

ized by two unusual properties: first the SHF confinement does not require introducing a defect lattice with the associated localized states at the fundamental or/and the second-harmonic frequencies; second, the location of the maximal SHF intensity is solely fixed by the position of the FF emitter. Despite this localization effect requires an unusual media, phase matched in all directions and presenting mixed left-hand- and right-handed behavior at both frequencies, we have demonstrated that these properties are encountered inside feasible 2D-PCs.

In conclusion, PC properties can overcome the classical physical limits of optical nonlinear processes. We have demonstrated a backward SHF localization effect, which occurs in perfect lattices and only depends on the emitter location inside the PC area. This localization mechanism needs an isotropic phase matched ω -LH/ 2ω -RH system. We have shown that GaN 2D-PCs behave as such a system in the visible second-harmonic regime (400–750 nm). Similar properties are expected for other nonlinear semiconductors ($\text{Al}_x\text{Ga}_{1-x}\text{As}$, for example) in hexagonal or other lattices. We think that this original approach opens interesting routes for the design of compact frequency converters.

-
- [1] *Photonic Band Gap Materials*, edited by C. M. Soukoulis, NATO Advanced Study Institute (Kluwer Academic, Dordrecht, 1996).
 - [2] E. Ozbay, K. Aydin, H. Caglayan, and K. Guven., *Photonics and Nanostructures Fundamentals and Applications* **2**, 87 (2004).
 - [3] T. Ishihara, K. Koshino, and H. Nakashima, *Phys. Rev. Lett.* **91**, 253901 (2003).
 - [4] J. P. Mondia *et al.*, *Opt. Lett.* **28**, 2500 (2003).
 - [5] F. Ren, R. Li, C. Cheng, H. Wang, J. Qiu, J. Si, and K. Hirao, *Phys. Rev. B* **70**, 245109 (2004).
 - [6] M. Liscidini and L. C. Andreani, *Phys. Rev. E* **73**, 016613 (2006).
 - [7] A. Di Falco, C. Conti, and G. Assanto, *Opt. Lett.* **31**, 250 (2006).
 - [8] C. Simonneau *et al.*, *Opt. Lett.* **22**, 1775 (1997).
 - [9] D. G. Gusev *et al.*, *Phys. Rev. B* **68**, 233303 (2003).
 - [10] Y. R. Shen, *The Principal of Nonlinear Optics* (Wiley, New York, 1984).
 - [11] J. Martorell, R. Vilaseca, and R. Corbolan, *Appl. Phys. Lett.* **70**, 702 (1997).
 - [12] M. Centini *et al.*, *Phys. Rev. E* **60**, 4891 (1999).
 - [13] J. Torres *et al.*, *Phys. Rev. B* **69**, 085105 (2004).
 - [14] Y. Dumeige *et al.*, *Phys. Rev. Lett.* **89**, 043901 (2002).
 - [15] V. M. Agranovich *et al.*, *Phys. Rev. B* **69**, 165112 (2004).
 - [16] I. V. Shadrivov, A. A. Zharov, and Y. S. Kivshar, *J. Opt. Soc. Am. B* **23**, 529 (2006).
 - [17] S. Foteinopoulou and C. M. Soukoulis, *Phys. Rev. B* **67**, 235107 (2003).
 - [18] S. Johnson and J. Joannopoulos, *Opt. Express* **8**, 173 (2001).
 - [19] N. Antoine-Vincent, *J. Appl. Phys.* **93**, 5222 (2003).
 - [20] S. Foteinopoulou and C. M. Soukoulis, *Phys. Rev. Lett.* **90**, 107402 (2003).
 - [21] E. Centeno and F. Felbacq, *J. Opt. Soc. Am. B* **23**, 2257 (2006).